Clim. Past Discuss., 8, 2145–2185, 2012
www.clim-past-discuss.net/8/2145/2012/
doi:10.5194/cpd-8-2145-2012

Climate of the Past Discussions

Cryogenic cave carbonate – a new tool for estimation of the Last Glacial permafrost depth of the Central Europe

K. Žák[1], D. K. Richter[2], M. Filippi[1], R. Živor[1], M. Deininger[3], A. Mangini[3], and D. Scholz[4,5]

[1]Institute of Geology AS CR, Prague, Czech Republic
[2]Institute for Geology, Mineralogy and Geophysics, Ruhr-University Bochum, Bochum, Germany
[3]Heidelberg Academy of Sciences, Heidelberg, Germany
[4]Institute for Geosciences, Johannes Gutenberg University Mainz, Mainz, Germany
[5]Max-Planck-Institute for Chemistry, Mainz, Germany

Received: 7 May 2012 – Accepted: 28 May 2012 – Published: 14 June 2012

Correspondence to: K. Žák (zak@gli.cas.cz)

Published by Copernicus Publications on behalf of the European Geosciences Union.

Abstract

Cryogenic cave carbonate (CCC) represents a specific type of speleothems, whose precipitation is triggered by freezing of mineralized karst water. Coarse-crystalline CCC, which formed during slow freezing of water in cave pools, is known in 20 Central European caves located in Germany, the Czech Republic, Slovakia and Poland. All these caves are situated in an area, which was glacier-free during the Weichselian. Whereas the formation of usual types of speleothems in caves of this region usually ceased during glacials, CCC precipitation was restricted to glacial periods. Since CCC represents a novel, useful paleoclimate proxy, data from Weichselian CCC occurrences in caves in Central Europe were collected, including their C and O stable isotope systematics, U-series ages and depth below the surface. When using only the CCC data from caves with limited cave ventilation, the permafrost depths of the Weichselian can be estimated to be at least 65 m in the lowlands and uplands. An isolated CCC find indicates that Weichselian permafrost penetrated to a depth of at least 285 m in the High Tatra Mts., Slovakia. A model of the formation of coarse-crystalline CCC assumes its formation especially during periods of permafrost thawing. U-series data confirm that permafrost depth changed and CCC precipitation occurred repeatedly in the studied area during Marine Isotope Stages 4, 3 and 2. One important phase of CCC formation related to permafrost thawing occurred between 40 and 21 ka BP, and the last phase of its formation was related to the final permafrost destruction between 17 and 12 ka BP.

1 Introduction

The southern limit of the continental glaciation of the central part of Europe during the Last Glacial (Weichselian) roughly followed the line defined by the present-day cities of Hamburg–Berlin–Poznań–Warszawa–Minsk (Poser, 1948; Svendsen et al., 2004). During the coldest phases of the Weichselian, a permafrost zone developed in the glacier-free area along the southern limit of the continental glacier (Vandenberghe, 2001; Czudek, 2005). Permafrost is defined as ground (rock or soil, including ice and/or organic material) that remains at or below 0 °C for at least two consecutive years (cf. Permafrost Subcommittee NRC Canada, 1988; Dobinski, 2011). For this glacier-free zone located between the northern continental and the Alpine mountain glaciations, little information has been available about the distribution, duration and thickness of permafrost during the Weichselian. It is usually assumed that continuous permafrost existed in the northern part of this zone during the Last Glacial Maximum (LGM), while discontinuous or sporadic permafrost was probably typical for more southerly located areas in the lowlands (Czudek, 2005).

Caves represent a subsurface environment, which has so far rarely been employed for estimation of past permafrost depths. The effects of past freezing temperatures in caves are indicated by several kinds of observations. Typical results of freezing temperatures include cave roof frost shattering, features produced by frost and ice action in unconsolidated cave sediments (i.e. various kinds of size-sorting phenomena and patterned ground phenomena), speleothem damage by frost and ice action, and other phenomena. These features have been described in several caves in Central Europe by numerous authors (Kyrle, 1929–1931; Kempe, 1989, 2004, 2008; Pielsticker, 1998, 2000; Wrede, 1999; Kempe and Rosendahl, 2003; Kempe et al., 2006). The main difficulty interpreting these observations results from the fact that some of these frost indicators can also be produced by other processes than frost and ice action. A further problem in relating them to surface climate change is represented by the difficulty in dating them. Probably the best evidence for former ice filling of cavities is represented by fragments of speleothems, called "ice attachments", attached by carbonate cement to steep sections of cave walls at sites where they could only be fixed due to the support of ice filling the cavity (or some other type of sediments filling the cavity at one time). These features were thoroughly studied in Germany (see references above) where extensive evidence of past ice filling of cavities has been collected.

Another indicator of past temperatures at the freezing point in caves is represented by cryogenic cave carbonate (CCC). CCC is generally formed by carbonate precipitation triggered by freezing of water. Salts are generally poorly soluble in ice, with solubility in the range of micro-moles or less (e.g. Gross et al., 1977; Petrenko and Withworth, 1999). Freezing of aqueous salt solutions, therefore, results in a process called salt (brine) rejection (for carbonate solutions, see Killawee et al., 1998). Freezing-induced segregation of solutes leads to a significant increase in the salt concentration in the residual (unfrozen) portion of the solution. As freezing proceeds, some dissolved compounds reach their saturation limit and precipitate as cryogenic minerals. Released gases either escape into the atmosphere or are concentrated in bubbles entrapped in the ice. Some other dissolved compounds (such as, e.g. Na^+ and Cl^-) form small inclusions of unfrozen, highly concentrated brine. These inclusions are usually distributed along ice crystal boundaries. The resulting ice is a complex multi-phase substance, which contains solid, liquid and gaseous phases (Mulvaney et al., 1988; Souchez and Lorrain, 1991).

CCC can be identified in caves based on its typical mode of occurrence and characteristic crystal and aggregate morphology. Its origin can be unequivocally confirmed by U-series dating fitting to glacial periods in combination with unique C and O stable isotope systematics (Žák et al., 2004, 2008; Richter and Riechelmann, 2008). Whereas the formation of conventional types of speleothems in caves in Central Europe typically ceases during glacials, CCC particularly forms during these periods, thus representing a unique new climate archive providing evidence for freezing conditions in subsurface. Except of caves, cryogenic carbonates occur commonly in numerous surface and near-surface environments, e.g. carbonates formed at the base of glaciers (subglacial calcite), in freezing groundwater springs (including naled, aufeis), in freezing lakes, in soils of cold environments, etc. These other types of cryogenic carbonates (reviewed in Žák et al., 2004) are not discussed in detail here.

The principal aim of this paper is to review the available data on the occurrence of CCC in deep caves in Central Europe and to significantly extend the existing CCC age determinations. The transfer of surface climate signal into caves hosting CCC is discussed, including the influence of cave ventilation. These data, in combination with

CPD
8, 2145–2185, 2012

the depth below the surface of each locality, are interpreted from the point of view of the Weichselian minimum permafrost depth penetration and periods of permafrost existence and destruction.

2 CCC and its environmental setting

CCC is found in caves in two modes of occurrence, representing two different types of environment of its formation. Fine-crystalline cryogenic carbonate powder, formed during rapid freezing of thin water layers in strongly ventilated caves or cave sections, is rather common. Typical environments for the formation of cryogenic carbonate powder are either cave entrances with seasonal water freezing and icicle formation, or ice caves in the temperate climatic zone, where low temperatures are maintained due to specific cave morphology with trapping of dense cold winter air. According to our knowledge, the first author who noted and properly explained the presence of CCC powder on the surface of seasonal icicles in entrance sections of caves in limestone karst was Kunský (1939). Since then, powdery cryogenic precipitate has been observed in cave entrances and ice caves by many authors (e.g. Viehmann, 1960; Ek and Pissart, 1965; Savchenko, 1976; Lauriol et al., 1988; Pulina, 1990; Clark and Lauriol, 1992, 2006a,b; Žák et al., 2004, 2008; Spötl, 2008; Lacelle et al., 2009; May et al., 2011). These powder CCC types, which form recently in strongly ventilated caves, are of no use for estimation of past permafrost depths.

The second mode of occurrence of CCC is represented by much larger crystals and crystal aggregates (ranging from <1 mm to about 40 mm), which were formed by segregation of the dissolved load during slow water freezing in pools. The recent formation of these coarse-crystalline CCC types has never been observed in caves. Coarse-crystalline CCC of clearly Holocene origin has been reported only once (Onac et al., 2011), as gledonite-like, up to 4 cm large aggregates found in the ice of the Scărişoara Ice Cave, Romania. The Weichselian coarse-crystalline CCC localities are known in 20 caves located on the territories of Germany, the Czech Republic, Slovakia and Poland. These specific carbonate forms have been recorded in caves in this area since the 1950's (Skřivánek, 1954; Tulis and Novotný, 1989; Urban and Złonkiewicz, 1989; Erlenmeyer and Schudelski, 1992; Schmidt, 1992; Durakiewicz et al., 1995) but their formation processes were not fully explained until the papers of Žák et al. (2004) and Richter and Niggemann (2005). Since then, coarse-crystalline CCC localities have been discovered in other caves in the periglacial zone of the Last Glacial in Europe (Orvošová and Žák, 2007; Richter and Riechelmann, 2007, 2008; Richter et al., 2008, 2009a,b,c, 2010a,b, 2011, 2012; Žák et al., 2008, 2011; Meissner et al., 2010). This specific type of speleothem frequently occurs in caves with limited or practically no ventilation. The only way how these cavities could have been cooled down to freezing conditions is, therefore, the occurrence of permafrost.

2.1 Morphology and mode of occurrence of coarse-crystalline CCC

Coarse-crystalline CCC usually occurs as accumulations of loose crystals and crystal aggregates freely deposited on the surface of the bottom of the cavity. CCC is only rarely covered by younger Holocene speleothems and/or clastic sediments. Its formation, therefore, represents one of the youngest events in the evolution of the studied caves. The accumulations (up to few cm thick, at maximum) usually cover an area of up to several square meters, located typically in the central parts of larger cavities, while they are usually not found in narrow corridors or near the cavity walls. CCC of this type never occurs near cave entrances or in a cave zone, which shows significant seasonal temperature changes. Instead, it is typically found in more remote cave sections.

The morphology of coarse-crystalline CCC is complex and differs from the usual secondary carbonate infillings and speleothems. The morphological variability led to development of many local terms used for description of CCC morphological types in individual countries. Generally, coarse-crystalline CCC types can be divided into several morphological, broadly-defined end-members, each with a typical position in the sequence of crystallization, and most probably slightly differing in the environment of their origin (see Sect. 2.2 for stable isotope data). Three most common morphological types include: (i) single crystals and their random or organized aggregates/intergrowth, (ii) crystalline raft-like aggregates, and (iii) fine- to coarse-crystalline spherical/globular forms.

The single crystals are usually small (from several tenths up to several millimeters) but relatively well-developed. Their stellate aggregates up to approximately 4 cm in size have also been documented (Urban and Złonkiewicz, 1989). More or less regular rhombohedra and, less frequently, scalenohedra are the most commonly detected crystal forms. The crystals are usually not perfectly developed, and various more or less skeletal-, hopper-, lathy-, fan-, serrated-forms and their various intergrowths are common. They are called “roses”, “wreaths” and “twigs” in the local literature (Durakiewicz et al., 1995).

Raft-like aggregates are characterized by their generally flat appearance and by crystal arrangements very similar to classical floating carbonate rafts in non-iced caves (cf. Hill and Forti, 1997, p. 88). The basic building elements of cryogenic rafts usually consist in calcite scalenohedra, sometimes elongated in the direction of the vertical axis. The size of these crystals varies from several tenths of micrometers to several millimeters. Crystals of two generations have been observed at some occurrences of cryogenic raft samples (Na Javorce Cave, Czech Republic, Žák et al., 2011).

Spherical or hemispherical forms representing the third type are described using various terms: “Zopfsinter” (Erlenmeyer and Schudelski, 1992), “hemispheres” (Tulis and Novotný, 1989; Forti, 1990), “cave caps” (Hill and Forti, 1997), or “cupula-spherolites” (Richter and Riechelmann, 2008). CCC of this type displays either smooth or fine to coarse crystalline surfaces and occurs as separate bodies or their random (sometimes planar) intergrowths/accumulations. It also often overgrows other types of coarse-crystalline CCC. Examples of the oriented intergrowth of two spherical bodies have also been documented. Visibly crystalline hemispheres (usually approximately half a sphere) with more or less exerted crystal edges and corners are usually formed of tightly intergrown, radially arranged crystals. Photographs of typical CCC field

CPD
8, 2145–2185, 2012

occurrences and the most common CCC crystal aggregate morphologies are contained in Supplement 1.

On the basis of the field observations, model of formation, and stable isotope studies (Žák et al., 2004), it seems highly probable that the sequence of formation of these aggregates starts with sharp-edge aggregate types composed of rhombohedra, while the smooth-surface types are formed later in the precipitation sequence. The CCC precipitation sequence is controlled by increasing bulk salinity of the residual unfrozen portion of the solution during progressive freezing and by slightly decreasing temperature. The isotopically most evolved type (showing the lowest $\delta^{18}O$ and highest $\delta^{13}C$ data within each site, see below in Sect. 2.2) formed during the final stage of freezing-induced crystallization is represented by more-or-less regular hemispheres. All these forms are today formed by low-Mg calcite. While the early rhombohedral and scalenohedral forms were probably already initially deposited as calcite, the smooth-surface types could have been originally formed by unstable carbonate phases like ikaite or vaterite (Killawee et al., 1998; Lacelle et al., 2009). They were probably all converted to calcite during the warmer Holocene climate.

2.2 C and O stable isotope systematics

Precipitation of carbonate minerals accompanied by water freezing exhibits large isotope fractionations, which have been frequently studied (Clark and Lauriol, 1992; Durakiewicz et al., 1995; Fairchild et al., 1996; Killawee et al., 1998; Žák et al., 2004, 2008, 2009, 2011; Richter and Niggemann, 2005; Lacelle et al., 2006, 2009; Lauriol et al., 2006a; Orvošová and Žák, 2007; Lacelle, 2007; Spötl, 2008; Richter et al., 2008, 2009a,b,c, 2010a,b; Richter and Riechelmann, 2007, 2008; Meissner et al., 2010; May et al., 2011; Onac et al., 2011). In the usual $\delta^{13}C$ vs. $\delta^{18}O$ plot, the data obtained on CCC samples cover a wide range from −2 to −24 ‰ in $\delta^{18}O$ and −11 to +17 ‰ VPDB in $\delta^{13}C$. Their variability is obviously much larger than the variability stable isotope data of speleothems, which do not form due to freezing conditions (Fig. 1). Possible isotope fractionations (probably very small or none) related to conversion from eventually originally present unstable carbonate phases to calcite are not known and, therefore, not evaluated.

The C and O isotope systematics of individual CCC types depends on the dominance of either disequilibrium (largely kinetic) or equilibrium isotope fractionation, which is controlled by the precipitation rate (cf. DePaolo, 2011). The precipitation rate is controlled by several partly inter-dependent factors, such as thickness/depth of the layer of freezing water, freezing rate, ventilation of the cave, etc. The kinetic isotope fractionations largely dominate during formation of the cryogenic carbonate powder. Rapid freezing of thin water films and ice sublimation both lead to a faster supersaturation of the carbonate solution and thus to higher precipitation rates. The stable isotope data trends of the CCC powder in the $\delta^{13}C$ vs. $\delta^{18}O$ diagram are similar to those for speleothems deposited during evaporation of water or during rapid kinetic degassing of CO_2 from the drip water (cf. Hendy, 1971; Mickler et al., 2006; Dreybrodt and Scholz, 2011). Nevertheless, during freezing-triggered precipitation of $CaCO_3$, the $\delta^{13}C$ values can reach very high values, commonly above +10 ‰ VPDB (Fig. 1).

In case of the coarse-crystalline CCC and slow water freezing in pools, the dominant factor controlling $\delta^{18}O$ values is equilibrium oxygen isotope fractionation between water and ice, which leads to progressive lowering of the oxygen isotope values ($\delta^{18}O_w$ values) of the residual, yet unfrozen solution (O'Neil, 1968; Jouzel and Souchez, 1982; Souchez and Jouzel, 1984). Kinetic isotope fractionation can occur during very rapid freezing and the resulting difference in $\delta^{18}O$ between liquid water and ice may be smaller than the equilibrium value (Souchez et al., 2000). The stable isotope data trends for coarse-crystalline CCC illustrated in Fig. 1 indicate that coarse-crystalline CCC $\delta^{18}O$ values reflect the $\delta^{18}O_w$ values. To achieve this, the precipitated carbonate needs to be in oxygen isotope equilibrium with H_2O. Hence the dissolved bicarbonate and carbonate ions (HCO_3^-, CO_3^{2-}) are in oxygen isotope equilibrium with H_2O, which is caused by the buffering reaction (Dreybrodt, 2008; Scholz et al., 2009; Dreybrodt and Scholz, 2011) – i.e. the oxygen isotope exchange between H_2O and HCO_3^-. According to Dreybrodt and Scholz (2011), at 0 °C it takes about 5.8 days for the oxygen isotope

CPD
8, 2145–2185, 2012

Title Page
Abstract | Introduction
Conclusions | References
Tables | Figures
◂| |▸
◂ ▸
Back | Close
Full Screen / Esc
Printer-friendly Version
Interactive Discussion

equilibration of HCO_3^- (approx. 98 % of equilibrium) with H_2O. From this it follows that the precipitation rate was very slow, because otherwise the oxygen isotope fingerprint of H_2O would be altered by isotope disequilibrium effects, and the isotope equilibrium fractionation probably occurred during the formation of coarse-crystalline CCC. The $\delta^{13}C$ vs. $\delta^{18}O$ plot indicates that $\delta^{13}C$ values are increasing whilst the $\delta^{18}O$ values are decreasing (cf. Fig. 1). This indicates that there are no carbon isotope reservoirs within the cavities and therefore the dissolved carbon ions becoming enriched in ^{13}C due to progressive carbonate precipitation. Stable isotope data trends in this direction in the $\delta^{13}C$ vs. $\delta^{18}O$ plot are generally rare in nature. CCC localities found in larger cavities usually exhibit higher $\delta^{13}C$ values than CCC localities occurring in smaller and more isolated cavities. Since coarse-grained CCC is formed under closed (or semi-closed) system conditions and cryogenic powders under open system conditions, the different stable isotope trends of these two types can be explained easily (Žák et al., 2008). The CCC is formed during changing $\delta^{18}O$ of the solution, the carbonate $\delta^{18}O$ data itself are not the carrier of paleoclimatic information. The paleoclimatic information of this novel archive is contained only in the presence of CCC (which is a proof of freezing temperature) at a given site and at a given moment of the past.

2.3 Regional distribution of the known CCC locations

Central European caves with occurrences of coarse-crystalline CCC are located in a belt defined by latitudes between 47°30′ and 51°30′ N and longitudes between 7°30′ and 20°30′ E. Details for all studied caves including the references to the original publications are listed in Table 1. The locations of the caves are also shown in Fig. 2. The entrance elevations are mostly in the range between 175 and 500 m a.s.l. (hilly regions). A small number of the studied caves are located in mountainous areas with entrance elevations between 690 and 2230 m a.s.l.

The studied caves are grouped in several karst regions. In Germany, a group of eight caves containing CCC is located in the “Rheinisches Schiefergebrige”, with morphologically complex caves formed mostly by corrosion in the phreatic or epiphreatic zone in Devonian limestone. Caves dominated by vadose morphology are less common here (represented by some parts of the Herbstlabyrinth-Advent Cave System). The entrance elevations of these caves are in the range from 175 to 501 m a.s.l. One German cave with CCC occurrence (Riesenberghöhle) is located in Jurassic limestone near the city of Hannover, and one mountain chasmal cave (Glaseishöhle), with an entrance elevation of 2230 m a.s.l., occurs in the Late Triassic limestone (Dachsteinkalk) of the Eastern Calcareous Alps (Fig. 2).

In the Czech Republic, the studied caves are mostly located in the Bohemian Karst, a small karst region developed in Silurian and Devonian limestone close to the city of Prague. CCC samples were collected here from four caves with entrance elevations between 244 and 402 m a.s.l. The caves in this region show a complex morphology (phreatic and/or epiphreatic maze caves are abundant). Several caves bear evidence of hydrothermal processes in the early phases of their evolution. One isolated locality in the Czech Republic (Javoříčko Caves, Fig. 2) with paleo-fluvial epipheratic to vadose levels is located in Devonian limestone in Central Moravia, with entrance elevations between 445 and 475 m a.s.l.

In Slovakia, the studied caves are generally located in the mountainous regions of the Western Carpathians and developed in several types of Mesozoic limestone. The entrance of morphologically complex and partly chasmal Hačova Cave, developed in Middle Triassic limestone, is at 690 m a.s.l. in the Lesser Carpathians, north of Bratislava. The other localities are found in mountain ranges with entrance elevations between 995 and 1 767 m a.s.l. In all of them, the CCC sites occur hundreds of meters away from the cave entrance.

In Poland, only one cave system with several CCC sites has so far been found. The extensive Jama Chelosiowa – Jasikinia Jaworznicka Cave System, located close to town of Kielce, contains at least twelve CCC occurrences. The caves are of complex phreatic and epiphreatic morphology and formed in Devonian limestone below a small hill in relatively flat country, partly covered by a thin blanket of clastic Early Triassic sediments. The cave entrances elevation ranges from 257 to 288 m a.s.l.

CPD
8, 2145–2185, 2012

Cross sections (side projections) of selected localities with the positions of CCC sites indicated are shown in Fig. 3. The figure compiles those localities, which contain the deepest known CCC sites and the caves discussed in more detail.

3 Materials and methods

Cave maps and cave sections were obtained from the original publications as well as local caving clubs. For construction of the cave sections, the surface morphology was derived from detailed topographical maps (scale 1:10 000). Both the cave maps and surface shape above the caves were in several cases verified or measured more precisely by the authors, using common mapping methods for underground and surface areas. Each of the known or newly discovered CCC sites was then indicated on the cave maps and sections. In order to show the relationships to the surface, the cave sections used are generally side projections (projected profiles), not extended profiles (cf. Palmer, 2007, p. 12). Depths (distances from the closest surface above the site) were then estimated from these cave sections. The CCC sites were field-documented and photo-documented. The C and O stable isotope data were collected from the original publications (see description of Fig. 1 for data sources).

^{230}Th/U-dating was performed both by thermal ionization mass spectrometry (TIMS) and by multi-collector inductively coupled plasma mass spectrometry (MC-ICPMS). TIMS samples were prepared similarly as described in Frank et al. (2000) or Schimpf et al. (2011). U-series isotopes were measured with an MAT 262 RPQ TIMS at the Heidelberg Academy of Sciences, Germany, using the double filament technique. MC-ICPMS samples were prepared similarly as described in Hoffmann et al. (2007) and analyzed at the Max-Planck-Institute for Chemistry (MPIC), Mainz, Germany. The mixed ^{233}U-^{236}U-^{229}Th spike used at MPIC was calibrated against a gravimetric U standard solution and a secular equilibrium standard solution. The gravimetric U standard solution was prepared from a NBL-112a metal bar and also used to calibrate the U-Th spike used at the Heidelberg Academy of Sciences (Hoffmann et al., 2007). The ^{229}Th

CPD
8, 2145–2185, 2012

concentration of the spike was calibrated against a secular equilibrium standard solution prepared from a 2 Ma old speleothem sample from Wilder Mann Cave, Austria (Meyer et al., 2009, 2011), which has been shown to be in secular equilibrium (Hoffmann et al., 2007). The calibration was checked using another secular equilibrium solution (Harwell Uraninite, HU) that was used to calibrate the U-Th spike used at the Heidelberg Academy of Sciences (Hoffmann et al., 2007). Analytical MC-ICPMS procedures involve a standard-sample bracketing procedure to derive correction factors for mass fractionation and Faraday cup to ion counter gain, similarly as described in Hoffmann et al. (2007) and Jochum et al. (2011).

All activity ratios reported for both laboratories were calculated using the decay constants from Cheng et al. (2000) and corrected for detrital Th assuming a bulk Earth $^{232}Th/^{238}U$ weight ratio of 3.8 for the detritus and ^{230}Th, ^{234}U and ^{238}U in secular equilibrium. All ages are reported in years BP, i.e. before the year 1950.

4 Results and discussion

Stable isotope data for individual coarse-crystalline CCC locations are shown in Fig. 1. The field relationships, i.e. the depth of the CCC sites below the closest surface, are presented on selected cave cross sections (Fig. 3), and are summarized in Table 1. Table 1 also contains all available U-series ages of the CCC sites, with the data sources identified. New TIMS and MC-ICPMS U-series data are presented in Tables 2 and 3, respectively.

4.1 Evidence for cryogenic origin of the CCC

All the studied CCC samples exhibit a typical mode of occurrence in the field, ranking them among very young events in the evolution of the studied caves (see Sect. 2). Hydrothermal origin or origin by disintegration of the host limestone is excluded by the unique morphology of the crystals and crystal aggregates.

The C and O stable isotope data for each locality exhibit a typical trend (Fig. 1) towards extremely low $\delta^{18}O$ values and slightly elevated $\delta^{13}C$ values as precipitation proceeds (see above in Sect. 2.2). The cryogenic origin of the studied samples can be considered as demonstrated. This is further confirmed by the determined U-series ages, which all (with one exception) suggest formation within glacials.

4.2 Ventilation of the studied caves

The typical environment of the occurrence of coarse-crystalline CCC is represented by cave sections remote from the entrances. Most caves with CCC occurrence are morphologically complex maze systems, open to the surface only via rather small entrances and/or very narrow and zigzag-shaped corridors. These caves maintain almost constant temperatures throughout the year, which are close to the present-day mean annual air temperature (MAAT). In several cases, the caves hosting CCC were discovered as isolated cavities by limestone quarrying, having no open connection to the surface (i.e. all connections were completely filled by pre-Weichselian sediments). In several other cases, the cavities hosting CCC were discovered by cavers digging through the pre-Weichselian sediments that originally completely filled the corridors. Cooling of these cavities to subzero temperatures by air circulation was impossible.

Only three localities are exceptions in this context. The chasmal Glasseishöhle (Northern Calcareous Alps) could have also been cooled by air exchange and not by permafrost evolution (present-day seasonal freezing inside the cave reaches a depth of 40 m, the CCC site occurs at a depth of 229 m). Recent temperatures slightly lower than the MAAT are also typical for the corridor hosting CCC in the Stratenská Cave System, Slovakia. This inclined corridor leads above the CCC site through a rock collapse in the direction towards a large collapse structure, which is open to the surface and accumulates dense cold air. Finally, stronger cave winds are also characteristic for some sections of Hačova Cave, Slovakia, but most of this cave (including the cavity hosting CCC) has recent temperatures close to the MAAT. In summary, for 17 of 20

CPD
8, 2145–2185, 2012

described sites, the only way to cool the cavities hosting the CCC was through evolution of permafrost.

4.3 Age and model of formation of the studied CCC

In total, 44 U-series ages on coarse-crystalline CCC are currently available (Table 1, Fig. 4). Of these 44 dates, 41 (i.e. more than 93 %) fall within the Weichselian between 104.0 and 11.9 ka BP. The age data are not distributed randomly within the Weichselian, but show several age clusters, containing commonly in one age cluster samples derived from different caves of the study area. Ages from the first half of the Weichselian are less frequent, since the colder part of the Weichselian started since approximately 70 ka BP (cf. Fig. 4). The oldest date within the Weichselian (104 ± 2.9 ka BP) falls into a relatively warm interval of Marine Isotope Stage (MIS) 5c. It was obtained for CCC sample from the Cold Wind Cave, Slovakia, located at a high elevation and at shallow depth below a mountain range. Dates from the first half of the Weichselian are more common for locations with higher elevation or with more northerly position within the study area (Cold Wind Cave, Slovakia; Jama Chelosiowa-Jaskinia Jaworznicka, Poland; Riesenberghöhle, Germany; see data in Table 1).

The period with the most frequent occurrence of CCC ages between ~40 and ~21 ka BP corresponds to the younger, climatically unstable part of the MIS 3 and the first part of MIS 2. It is expected that this climatically unstable period induced oscillations in the permafrost depth, creating conditions suitable for CCC formation. CCC age data corresponding to the Last Glacial Maximum (LGM; ~26 to ~19 ka BP; Clark et al., 2009) are generally scarce, and are only represented by ages for the Stratenská Cave, Slovakia. Stratenská Cave is one of three caves within the studied set, which could have also been cooled by air circulation. Another important group of dated samples from several caves is represented by ages between 17.0 and 11.9 ka BP, corresponding to periods of variable climate after the LGM and before the beginning of the Holocene when the permafrost thickness was generally decreasing.

CPD
8, 2145–2185, 2012

Of the total data set of 44 age determinations, only three (less than 7 %) do not fit into the Weichselian. Two older dates (Apostelhöhle, Germany, 408^{+42}_{-31} ka BP; Cold Wind Cave, Slovakia, 180 ± 6.3 ka BP) fit into the younger parts of the Elsterian and Saalian glacials, respectively. Findings of CCC from earlier glacials are rare, probably because these old CCC was covered during later cave evolution by clastic sediments or flowstone. From the whole data set, only one date corresponds to Holocene age (9.191 ± 0.072 ka BP; Na Javorce Cave, Bohemian Karst). This outlier may be interpreted in two ways. Either the U-series system of the sample was not closed (and the sample post-depositionally adsorbed U during the Holocene; the $^{234}U/^{238}U$ activity ratio of this sample is by far the highest in the whole data set), or the sample age indeed indicates the existence of relic permafrost in the Early Holocene. The first interpretation is supported by the sample character (aggregates of relatively small crystals with large surface area), the second by the position of the sampling site, which is the deepest (65 m below surface) within the low altitude localities.

Comparison of the U-series ages with the benthic $\delta^{18}O$ stack from Lisiecki and Raymo (2005) and with NGRIP climate record (North Greenland Ice Core Project Members, 2004) is shown in the Fig. 4. The CCC ages mostly plot near transitions from colder to warmer periods. This is in agreement with the published models of the formation of ice fill in cavities during permafrost (Pielsticker, 2000) and CCC formation in these cavities (Richter and Riechelmann, 2008; Richter et al., 2010b). Deeper infiltration of groundwater is practically impossible during permafrost growth since infiltration is eliminated due to blocking by ice. Groundwater movement is mostly restricted to the near-surface permafrost layer during these periods.

Deeper circulation of either highly mineralized groundwater within the permafrost or common groundwater in taliks is possible in karst environments (Ford and Williams, 2007, 421–427 pp.; Spektor and Spektor, 2009). Some karst conduits can be kept open by seasonally flowing water, transporting heat into the permafrost zone. Water with higher mineralization can flow within the permafrost at temperatures significantly below 0 °C. In Canada at 79° N, Pollard et al. (1999) documented perennial discharge

CPD
8, 2145–2185, 2012

of mineralized saline groundwater with a temperature of $-4\,^{\circ}$C. Nevertheless, the available age data show that the periods of permafrost propagation to greater depths were usually not associated with intensive CCC formation.

In contrast, the upper limit (0 °C isotherm) of the relic permafrost is lowered during the permafrost thawing. Thawing propagates to depth more rapidly along water-conducting clefts and karst channels. Because the zone above the upper limit of the deep relic permafrost is water-rich when a karst channel with liquid water penetrates into the top of a cavity, liquid water relatively rapidly fills the whole cavity. The cavity itself, however, is still in the permafrost zone. The water freezes slowly here (cf. Pielsticker, 2000, who came to an identical conclusion from the thermal modeling). The duration of the ice fill of the cavity is, therefore, only a short-term event. As the 0 °C isotherm moves deeper, the ice melts and CCC crystals and crystal aggregates are freely deposited on the bottom of the cavity. The CCC age data show that, depending on the oscillation of the surface climate, the permafrost depth oscillated during the Weichselian. One important period of repeated permafrost growth and destruction occurred between 40 and 21 ka BP, and the final permafrost destruction (at the depths of the studied caves) followed between 17.0 and 11.9 (possibly 9.2) ka BP. The basic principle of CCC formation in a cavity is depicted on the simple general model in Fig. 5. However, it is clear that for some of the studied caves more complex scenarios may be constructed, with repetition of water freezing periods (see Richter et al., 2010a) or possibly freezing of water streams and lakes in caves of the vadose type (see Richter et al., 2011).

4.4 Estimation of past permafrost thickness

Discontinuous permafrost typically starts to develop in areas with MAAT below approximately 1 °C (King, 1984). Continuous permafrost is typical for areas with subzero MAAT. Its depth penetration can be roughly calculated based on MAAT, using appropriate equations (e.g. French, 2007; Anderson and Anderson, 2010). Nevertheless, these model calculations represent only a rough estimate since the real permafrost thickness depends also on many other parameters such as thermal conductivity and diffusivity

Discussion Paper | Discussion Paper | Discussion Paper | Discussion Paper |

CPD

8, 2145–2185, 2012

Cryogenic cave carbonate

K. Žák et al.

of earth materials, vegetation cover, quantity and duration of snow cover, topography including the aspect, which influences the intensity of insulation or existence of water bodies at the surface (French, 2007).

An important factor for permafrost depth penetration is the duration of the climatic period with subzero MAAT. Construction and destruction (thawing) of deep permafrost is usually substantially delayed with respect to the evolution of the surface climate. Full thermal equilibration of the upper crust to the new surface climate conditions may take several thousand years (Šafanda and Rajver, 2001). Temperature-depth profiles measured in deep boreholes in the area of past permafrost still exhibit thermal relics of the Weichselian permafrost in Europe even today (Šafanda and Rajver, 2001; Šafanda et al., 2004). A deep relic zone with temperature close to 0 °C starting at a depth of 357 m below the surface and continuing down to the borehole base (450 m) was reported by Honczaruk and Śliwiński (2011) and Szewczyk and Nawrocki (2011) in Cretaceous sediments of North-eastern Poland. The temperature is controlled by water/ice transitions here.

Today, in Central Europe, permafrost exists at higher elevations in the Alps and sporadic permafrost patches are also assumed to exist in the highest parts of the Western Carpathians (High and Low Tatra Mts.) in the territory of Poland and Slovakia (Brown et al., 1997; Keller et al., 1998; Dobiński, 2005). Recent permafrost in European mountain regions is generally more irregular than the permafrost, which developed in lowlands during glacials. In the Alps, the lower limit of occurrence of recent sporadic permafrost is at approximately 2100 m a.s.l., and discontinuous permafrost starts here at approx. 2400 m a.s.l. (e.g. Keller et al., 1998). Sporadic or discontinuous permafrost is probably also present in the Tatra Mts. at elevations above approximately 1930 m a.s.l., but has so far been indicated only by ground-surface temperature measurement and ground-penetrating radar on the northern mountain slopes (e.g. Gadek and Grabiec, 2008). The present-day climate-related change of permafrost in Europe was studied by Harris et al. (2003, 2009).

The deepest cavities hosting CCC in the "Rheinisches Schiefergebrige" (Germany) and in the Bohemian Karst (western part of the Czech Republic) are at similar depths of 60 to 65 m below the surface. The data do not allow estimating whether the permafrost was discontinuous or continuous. The depth of 65 m can be considered as the minimum permafrost depth during the second half of the Weichselian in this area. Since the formation of CCC occurs predominantly during permafrost destruction, which certainly proceeds both from above and from below, the maximum permafrost depth was certainly greater. It should also be noted that the permafrost depth is typically lower in karst areas than the surrounding non-karst areas (Ford and Williams, 2007). One site in the Northern Calcareous Alps exhibits CCC at a depth of 229 m below the entrance (entrance elevation of 2230 m a.s.l.). Based on unpublished modeling (V.T. Balobayev and L. I. Schipiciny in Czudek, 2005), the maximum Weichselian permafrost depth of the Czech Republic was estimated to be in the range from approximately 50 to maximally 250 m, which is in agreement with our CCC depth data.

In the eastern part of the Czech Republic (Moravia), only one locality is known with CCC occurrence at the relatively shallow depth of 30 m below the surface (Javoříčko Caves). The cavity where the CCC occurs also hosts other indications of former ice fill (e.g. destroyed speleothems and "ice-attachments"). In the large cave systems of the slightly more southerly located Moravian Karst, no CCC site is known. This CCC absence could possibly be due to the existence of abundant underground water streams in this karst region, which could produce extensive taliks. Relatively thick permafrost in the northern part of Moravia is indicated by the observation of Růžičková and Zeman (1992), who described post-cryogenic structures down to a depth of 220 m in the Blahutovice borehole. Unfortunately, this observation is not accompanied by dating and, so it is not clear when the observed features were formed.

All the sites in Slovakia are located in mountainous areas. Greater depths for the CCC sites can be expected here since even today some of these caves exhibit relatively low temperatures. The deepest CCC site in Mesačný Tieň Cave in the High Tatra Mts. is located at a depth of 285 m (surface elevation approx. 1800 m a.s.l.). The

CPD
8, 2145–2185, 2012

present-day temperature of the cave interior varies between 1.0 and 3.5 °C (personal communication by B. Šmída; no more precise temperature measurements have been performed to date; the whole cave system was explored after 2004). This deep occurrence of CCC is in agreement with earlier estimates of Weichselian permafrost depth for the High Tatra Mts., with potential Weichselian permafrost depths down to 400 m below the surface (Dobiński, 2004).

4.5 Further interpretation possibilities for CCC data

Since the formation of CCC proceeds at 0 °C (or slightly below, if the residual solution becomes more mineralized), the data allow direct calculation of the corresponding $\delta^{18}O_w$ values of the water from which the carbonate was formed. As stated in Sect. 2.2, the $\delta^{18}O_w$ values of the residual, yet unfrozen portion of the solution are shifted to progressively lower values during freezing. Therefore, calculation using the temperature of 0 °C and the highest observed CCC $\delta^{18}O$ value yields the $\delta^{18}O_w$ value closest to the initial value at the onset of freezing.

The calculation is further complicated by rather imprecise calibration of the oxygen isotope fractionation between carbonate and water at 0 °C. The calculations using published calcite/water oxygen isotope fractionations at 0 °C differ by several ‰. For this calculation exercise, we use the equation of Friedman and O'Neil (1977), which suggests a calcite-water fractionation of 34.37 ‰ at 0 °C . Since the $\delta^{18}O_w$ value changes during freezing, the calculated data represent only the unilateral limit of the initial $\delta^{18}O_w$ value. This model calculation shows that the $\delta^{18}O_w$ value of Weichselian karst water from which the CCC started to grow was around −15 ‰ VSMOW in the lowlands and uplands, and around −20 ‰ VSMOW in the studied mountain regions.

Formation of CCC at 0 °C offers some other analytical and interpretation possibilities. During the last few years, preliminary application of "clumped isotope thermometry" has been started (see the recent review by Eiler, 2011). Since the formation of CCC proceeds by slow precipitation of $CaCO_3$ probably under conditions of isotopic

CPD
8, 2145–2185, 2012
Cryogenic cave carbonate
K. Žák et al.

equilibrium at a temperature around 0 °C by purely inorganic precipitation without any biological effects, CCC may be particularly useful for the calibration of the clumped isotope thermometer at low temperatures.

5 Conclusions

Cryogenic cave carbonate (CCC) formed by expulsion of the dissolved load during slow water freezing in caves during the Last Glacial (Weichselian) has been found in 20 caves located in the territories of Germany, the Czech Republic, Slovakia and Poland. The caves were located in the glacier-free zone between the northern continental glaciation and the Alpine mountain glaciation during the Weichselian. The CCC formed mainly in several restricted time periods, mostly between 40 and 21 ka BP and 17.0 and 12 ka BP. CCC formation in deep caves mostly occurred during periods of permafrost thawing related to surface within-glacial warming periods (interstadials), when liquid water penetrated into empty cavities within the deeper relic permafrost and froze slowly. The CCC occurrences indicate the minimum permafrost depth during the younger half of the Weichselian in the studied area to be more than 65 m in the lowlands and uplands. In the High Tatra Mts., a permafrost depth of more than 285 m below surface is suggested.

Since CCC is formed at a temperature of 0 °C or slightly less, they offer other, yet unexplored interpretation possibilities, such as estimates of the $\delta^{18}O$ values of the source water or calibrations of "clumped isotope thermometry" at low temperatures.

Supplementary material related to this article is available online at: http://www.clim-past-discuss.net/8/2145/2012/cpd-8-2145-2012-supplement.pdf.

CPD
8, 2145–2185, 2012

Acknowledgements. This paper is based on research performed in project GA P210/10/1760 of the Czech Science Foundation, with further support from the AV0Z30130516 research program and the Daphne DFG-FG 668 project. D. Scholz is thankful to K. P. Jochum and M. Andreae, MPIC, Mainz, for providing analytical facilities and B. Schwager for assistance during sample preparation. The authors are grateful to local cavers for their assistance and accompanying us in the caves during field documentation and sampling, and for providing us with cave maps and sections (Germany: I. Dorsten, S. Niggemann, U. Polikeit, A. Schudelski, S. Voigt; Czech Republic: J. Dragoun, S. Komaško, J. Novotný, J. Vejlupek, S. Vybíral, J. Zelinka; Slovakia: M. Budaj, S. Mudrák, B. Šmída, M. Štéc, J. Tulis; the assistance of B. Šmída, who prepared unpublished sections of Hačova and Mesačný Tieň caves, was especially appreciated).

References

Anderson, R. S. and Anderson, S. P.: Periglacial processes and forms, in: Geomorphology, the Mechanics and Chemistry of Landscapes, Cambridge University Press, Cambridge, UK, 270–303, 2010.

Brown, J., Ferrians, H. M, Heginbottom, J. A., and Melnikov, E. S.: Circum-arctic map of the permafrost and ground-ice conditions, Map CP-45, Circum-Pacific map series, USGS, Washington, D.C., USA, 1997.

Cheng, H., Edwards, R. L., Hoff, J., Gallup, C. D., Richards, D. A., and Asmeron, Y.: The half-lives of uranium-234 and thorium-230, Chem. Geol., 169, 17–33, 2000.

Clark, I. D. and Lauriol, B.: Kinetic enrichment of stable isotopes in cryogenic calcites, Chem. Geol., 102, 217–228, 1992.

Clark, P. U., Dyke, A. S., Shakun, J. D., Carlson, A. E., Clark, J., Wohlfarth, B., Mitrovica, J. X., Hostetler, S. W., and McCabe, A. M.: The Last Glacial Maximum, Science, 325, 710–714, 2009.

Czudek, T.: Quaternary development of landscape relief in the Czech Republic, Moravian Museum, Brno, 238 pp., 2005.

DePaolo, D. J.: Surface kinetic model for isotopic and trace element fractionation during precipitation of calcite from aqueous solutions, Geochim. Cosmochim. Acta, 75, 1039–1056, 2011.

Dobiński, W.: Permafrost in the Tatra Mts.: genesis, features, evolution, Przeglad Geograficzny, 76, 327–343, 2004.
Dobiński, W.: Permafrost of the Carpathian and Balkan Mountains, Eastern and Southeastern Europe, Permafrost Periglac., 16, 395–398, 2005.
Dobinski, W.: Permafrost, Earth Sci. Rev., 108, 158–169, 2011.
Dragoun, J., Vejlupek, J., and Novotný, J.: Jeskyně Na Javorce, propast Žbluňk, Speleofórum, 30, 21–24, 2011.
Dreybrodt, W.: Evolution of the isotopic composition of carbon and oxygen in calcite precipitating H_2O-CO_2-$CaCO_3$ solution and the related isotopic composition of calcite in stalagmites, Geochim. Cosmochim. Acta, 72, 4712–4724, 2008
Dreybrodt, W. and Scholz, D.: Climatic dependence of stable carbon and oxygen isotope signals recorded in speleothems: from soil water to speleothem calcite, Geochim. Cosmochim. Acta, 75, 734–752, 2011.
Durakiewicz, T., Haas, S., Migaszewski, M., and Urban, J.: Origin of "calcite groats" in the Chelosiowa Cave near Kielce (Holy Cross Mts.) inferred from petrographic and isotopic investigations, Geol. Q., 39, 75–94, 1995.
Eiler, J. M.: Paleoclimate reconstruction using carbonate clumped isotope thermometry, Quaternary Sci. Rev., 30, 3575–3588, 2011.
Ek, C. and Pissart, A.: Depôt de carbonate de calcium par congélation et teneur en bicarbonate des eaux résiduelles, Acad. Sci. Paris Comptes Rendus, 260, 929–932, 1965.
Erlenmeyer, M. and Schudelski, A.: Der Malachitdom und die anderen Höhlen im Steinbruch Düstertal, in: Der Malachitdom, ein Beispiel interdisziplinärer Höhlenforschung im Sauerland, Geologisches Landesamt Nordrhein-Westfalen, Krefeld, 39–68, 1992.
Fairchild, I. J., Killawee, J. A., Spiro, B., and Tison, J.-L.: Calcite precipitates formed by freezing processes: kinetic controls on morphology and geochemistry, in: Proceedings Fourth International Symposium on the Geochemistry of Earth's Surface, Ilkley, England, 178–183. 1996.
Ford, D. and Williams, P.: Karst Hydrogeology and Geomorphology, John Wiley & Sons, New York, 562 pp., 2007.
Forti, F.: La grotta Malachitdom: un ambiente mineralogicoeccezionale che rischia di andare distrutto, Riv. Ital. Mineral. Paleontol., 67, 3–7, 1990.

Frank, N., Braum, M., Hambach, U., Mangini, A., and Wagner, G.: Warm period growth of travertine during the last interglacial in Southern Germany, Quaternary Res., 54, 38–48, 2000.

French, H. M.: The Periglacial Environment, John Wiley & Sons, Chichester, 458 pp., 2007.

Friedman, I. and O'Neil, J. R.: Compilation of stable isotope fractionation factors of geochemical interest, US Geol. Surv. Prof. Pap., 440-KK, 49 pp., 1977.

Gadek, B. and Grabiec, M.: Glacial ice and permafrost distribution in the Medena Kotlina (Slovak Tatras): mapped with application of GPR and GST measurements, Studia Geomorphologica Carpatho Balcanica, 42, 5–22, 2008.

Gross, G. W., Wong, P. M., and Humes, K.: Concentration dependent solute redistribution at the ice-water phase boundary, III. Spontaneous convection, Chloride solutions, J. Chem. Phys., 67, 5264–5274, 1977.

Harris, C., Vonder Mühll, D., Isaksen, K., Haeberli, W., Sollid, J. L., King, L., Holmlund, P., Dramis, F., Guglielmin, M., and Palacios, D.: Warming permafrost in European mountains, Global Planet. Change, 39, 215–225, 2003.

Harris, C., Arenson, L. U., Christiansen, H. H., Etzelmüller, B., Frauenfelder, R., Gruber, S., Haeberli, W., Hauck, C., Hölzle, M., Humlum, O., Isaksen, K., Kääb, A., Kern-Lütschg, M. A., Lehning, M., Matsuoka, N., Murton, J. B., Nötzli, J., Phillips, M., Ross, N., Seppälä, M., Springman, S. M., and Vonder Mühll, D.: Permafrost and climate in Europe: monitoring and modelling thermal, geomorphological and geotechnical responses, Earth Sci. Rev., 92, 117–171, 2009.

Hendy, C. H.: The isotopic geochemistry of speleothems, I. The calculation of the effects of different modes of formation and the isotope composition of speleothems and their applicability as palaeoclimatic indicators, Geochim. Cosmochim. Acta, 35, 801–824, 1971.

Hill, C. A. and Forti, P.: Cave Minerals of the World, 2nd Edn., National Speleological Society, Huntsville, Alabama, USA, 463 pp., 1997.

Hoffmann, D. L., Prytulak, J., Richards, D. A., Elliott, T., Coath, C. D., Smart, P. L., and Scholz, D.: Procedures for accurate U and Th isotope measurements by high precision MC-ICPMS, Int. J. Mass Spectrom., 264, 97–109, 2007.

Honczaruk, M. and Śliwiński, Ł.: Results of hydrogeological research of the deep permafrost zone in the Udryń PIG 1 borehole, Biuletyn Państwowego Instytutu Geologicznego, 445, 203–216, 2011.

Jochum, K. P., Wilson, S. A., Abouchami, W., Amini, M., Chmeleff, J., Eisenhauer, A., Hegner, E., Iaccheri, L. M., Kieffer, B., Krause, J., McDonough, W. F., Mertz-Kraus, R., Raczek, I., Rudnick, R. L., Scholz, D., Steinhoefel, G., Stoll, B., Stracke, A., Tonarini, S., Weis, U., and Woodhead, J. D.: GSD-1G and MPI-DING Reference Glasses for in situ and bulk isotopic determination, Geostand. Geoanal. Res., 35, 193–226, 2011.

Jouzel J. and Souchez R. A.: Melting-refreezing at the glacier sole and the isotopic composition of the ice, J. Glaciol., 28, 35–42, 1982.

Keller, F., Frauenfelder, R., Gardaz, J.-M., Hoelzle, M., Kneisel, C., Lugon, R., Phillips, M., Reynard, E., and Wenker, L.: Permafrost map of Switzerland, Proceedings Permafrost – Seventh International Conference, Yellowknife, Collection Nordiciana, 55, 557–562, 1998.

Kempe, S.: Sinterschäden verursacht durch Permafrost or Erdbeben?, Mitteilungen des Verbandes der deutschen Höhlen- und Karstforscher e. V. München, 35, 87–90, 1989.

Kempe, S.: Natural speleothem damage in Postojnska Jama (Slovenia), caused by glacial cave ice?, Acta Carsologica, 33, 265–289, 2004.

Kempe, S.: Natürliche Sinterschäden, Indikatoren für glaziales Höhleneis in Mitteleuropa, Stalactite, 58, 39–42, 2008.

Kempe, S. and Rosendahl, W.: Speleothem damage in Central European Caves, a result of permafrost processes?, Proceedings Climate Changes: the Karst Record III, 3rd International Conference, Montpellier, France, 11–14 May 2003, 88–89, 2003.

Kempe, S., Doeppes, D., Bauer, I., Dirks, H., Dorsten, I., Hueser, A., and Eisenhauer, A.: Naturally damaged speleothems, indicators of glacial cave ice in Central Europe, Karst Waters Institute Special Publication, Charles Town, West Virginia, USA, 10, p. 35, 2006.

Killawee, J. A., Fairchild, I. J., Tison, J.-L., Janssen, L., and Lorrain, R.: Segregation of solutes and gases in experimental freezing of dilute solutions: Implications for natural glacial systems, Geochim. Cosmochim. Acta, 62, 3637–3655, 1998.

King, L.: Permafrost in Skandinavien. Untersuchungsergebnisse aus Lappaland, Jotunheimen und Dovre/Rondane, Heidelberger geographische Arbeiten, 76, 1–174, 1984.

Kunský, J.: Některé formy ledových krápníků, Rozpravy I I. Třídy České akademie, 49, 1–8, 1939.

Kyrle, G.: Frostsprengungen im Höhlensinter, Speläol. Jb., 11/12, 134–136, 1929–1931.

Lacelle, D.: Environmental setting (micro)morphologies and stable C-O-isotope composition of cold climate carbonate precipitation, A review and evaluation of their potential as paleoclimatic proxies, Quaternary Sci. Rev., 26, 1670–1689, 2007.

Lacelle, D., Lauriol, B., and Clark, I. D.: Effect of chemical composition of water on the oxygen-18 and carbon-13 signature preserved in cryogenic carbonates, Arctic Canada: implications in paleoclimatic studies, Chem. Geol., 234, 1–16, 2006.

Lacelle, D., Lauriol, B., and Clark, I. D.: Formation of seasonal ice bodies and associated cryogenic carbonates in Caverne de l'Ours, Québec, Canada: kinetic isotope effects and pseudo-biogenic crystal structures, J. Cave Karst Stud., 71, 48–62, 2009.

Lauriol, B., Carrier, L., and Thiebaudeau, P.: Topoclimatic zones and ice dynamics in the caves of the Northern Yukon, Canada, Arctic, 41, 215–220, 1988.

Lauriol, B., Lacelle, D., and Clark, I. D.: Carbonate powders in freezing caves, 2nd International Workshop on Ice Caves (IWIC-II), Demänovská Dolina, Slovak Republic, 8–12 May 2006, Volume of Abstracts, 13, 2006a.

Lauriol, B., Prévost, C., and Lacelle, D.: The distribution of diatom flora in ice caves of the Northern Yukon Territory, Canada: relationship to air circulation and freezing, Int. J. Speleol., 35, 83–92, 2006b.

Lisiecki, L. E. and Raymo, M. E.: A Pliocene-Pleistocene stack of 57 globally distributed benthic $\delta^{18}O$ records, Paleooceanography, 20, 1–17, 2005.

May, B., Spötl, C., Wagenbach, D., Dublyansky, Y., and Liebl, J.: First investigations of an ice core from Eisriesenwelt cave (Austria), The Cryosphere, 5, 81–93, doi:10.5194/tc-5-81-2011, 2011.

Meissner, P., Richter, D. K., and Immenhauser, A.: Cryogenic calcites in caves of the Rhenish Slate Mountains – a new proxy for palaeoclimate reconstructions?, SDGG Heft, 68, 385, Darmstadt, 2010.

Meyer, M. C., Cliff, R. A., Spötl, C., Knipping, M., and Mangini, A.: Speleothems from the earliest Quaternary: Snapshots of paleoclimate and landscape evolution at the northern rim of the Alps, Quaternary Sci. Rev., 28, 1374–1391, 2009.

Meyer, M. C., Cliff, R. A., and Spötl, C.: Speleothems and mountain uplift, Geology, 39, 447–450, 2011.

Mickler, P. J., Stern, L. A., and Banner, J. L.: Large kinetic isotope effects in modern speleothems, Geol. Soc. Am. Bull., 118, 65–81, 2006.

Mulvaney, R., Wolff, E. W., and Oates, K.: Sulphuric acid at grain boundaries in Antarctic ice, Nature, 331, 247–249, 1988.

North Greenland Ice Core Project Members: High-resolution record of Northern Hemisphere climate extending into the last interglacial period, Nature, 431, 147–151, 2004.

O'Neil, J. R.: Hydrogen and oxygen isotope fractionation between ice and water, J. Phys. Chem., 72, 3683–3684, 1968.

Onac, B. P., Wynn, J. G., and Citterio, M.: Ikaite in the Scarisoara Ice Cave (Romania): origin and significance, Geophysical Research Abstracts, 13, EGU2011-5188, 2011.

Orvošová, M. and Vlček, L.: Nové nálezy kryogénnych jaskynných karbonátov (New finds of the cryogenic cave carbonates), Bull. Slovak Speleol. Soc., 43, 58–64, 2012.

Orvošová, M. and Žák, K.: Cryogenic carbonate precipitation in caves: Jaskyňa Studeného Vetra Cave (Low Tatras, Slovakia) case study, Karst and Cryokarst, 25th Speleological School and 8th GLACKIPR Symposium, Sosnowiec, Wrocław, Poland, Guidebook & Abstracts, 104–105, 2007.

Palmer, A. N.: Cave Geology, Cave Books, Dayton, 454 pp., 2007.

Permafrost Subcommittee, National Research Council of Canada: Glossary of permafrost and related ground-ice terms, National Research Council of Canada Technical Memorandum No. 142, Ottawa, Ontario, Canada, 156 pp., 1988.

Petrenko, V. F. and Withworth, R. W.: Physics of Ice, Oxford University Press, Oxford, 390 pp., 1999.

Pielsticker, K.-H.: Die Große Sunderner Höhle, Sundern, Hochsauerlandkreis, BRD, Sinterbrüche und Umlagerungen, Eisdruck oder Erdbeben, Mitteilungen des Verbandes der deutschen Höhlen- und Karstforscher e. V. München, 44, 4–11, 1998.

Pielsticker, K.-H.: Höhlen und Permafrost – Thermophysikalische Prozesse von Höhlenvereisungen während des Quartärs, Bochumer Geol. Geotech. Arbeit., 55, 187–196, 2000.

Pollard, W., Omelon, C., Andersen, D., and McKay, C.: Perennial spring occurrence in the Expedition Fiord area of Western Axel Heiberg Island, Canadian High Arctic, Can. J. Earth Sci., 36, 105–120, 1999.

Poser, H.: Boden- und Klimaverhältnisse in Mittel- und Westeuropa während der Würmeiszeit, Erdkunde, 2, 53–68, 1948.

Pulina, M.: Geomorphological effects of the cryochemical process, Quaestiones Geographicae, 13/14, 99–112, 1990.

Richter, D. K. and Niggemann, S.: Kryogene Calcite in Höhlen des Rheinischen Schiefergebirges, Mitteilungen des Verbandes der deutschen Höhlen- und Karstforscher, München, 51, 129–132, 2005.

Richter, D. K. and Riechelmann, D. F. C.: Cupulas of the Malachitdom cave (Sauerland/NRW) – cryogenic spherolites with unusual calcitic structure and C/O-isotopic composition, Geo. Alp, 4, p. 79, 2007.

Richter, D. K. and Riechelmann, D. F. C.: Late Pleistocene cryogenic calcite spherolites from the Malachitdom Cave (NE Rhenish Slate Mountains, Germany): origin, unusual internal structure and stable C-O isotope composition, Int. J. Speleol., 37, 119–129, 2008.

Richter, D. K., Neuser, R. D., and Voigt, S.: Kryogene Calciumpartikel aus der Heilenbecker Höhle in Ennepetal (NE Bergisches Land/Nordrhein-Westfalen) (Cryogenic calcite particles from the Heilenbecker Cave in Ennepetal, NE Bergisches Land/North-Rhine Westphalia), Die Höhle, 59, 37–47, 2008.

Richter, D. K., Dreyer, R., Niggemann, S., and Pielsticker, K.-H.: Kryokalcite in der Großen Sunderner Höhle (Sauerland) – ein weiterer Beleg für die vormalige Eishöhle, Mitteilungen des Verbandes der deutschen Höhlen- und Karstforscher e. V. München 55, 80–85, 2009a.

Richter, D. K., Mangini, A., and Voigt, S.: Erste Th/U-datierte Kryocalcite der mittleren Weichsel-eiszeit aus einer Höhle des Rheinischen Schiefergebirges (Heilenbecker Höhle, Bergisches Land), Mitteilungen des Verbandes der deutschen Höhlen- und Karstforscher e. V. München, 55, 125–127, 2009b.

Richter, D. K., Voigt, S., and Neuser, R. D.: Kryogene Calcite unterschiedlicher Kristallform und Kathodolumineszenz aus der Glaseishöhle am Schneiber (Steinernes Meer/Nationalpark Berchtesgaden, Deutschland), Die Höhle, 60, 3–9, 2009c.

Richter, D. K., Meissner, P., Immenhauser, A., Schulte, U., and Dorsten, I.: Cryogenic and non-cryogenic pool calcites indicating permafrost and non-permafrost periods: a case study from the Herbstlabyrinth-Advent Cave system (Germany), The Cryosphere, 4, 501-509, doi:10.5194/tc-4-501-2010, 2010a.

Richter, D. K., Schulte, U., Mangini, A., Erlenmeyer, A., and Erlenmeyer, M.: Mittel- und oberpleistozäne Calcitpartikel kryogener Entstehung aus der Apostelhöhle südöstlich Brilon (Sauerland, NRW), Geologie und Paläontologie in Westfalen, 78, 61–71, 2010b.

Richter, D. K., Mischel, S., Dorsten, I., Mangini, A., Neuser, R. D., and Immenhauser, A.: Zerbrochene Höhlensinter und Kryocalcite als Indikatoren für eiszeitlichen Permafrost im Herbstlabyrinth-Adventhöhle-System bei Breitscheid-Erdbach (N-Hessen), Die Höhle, 62, 31–45, 2011.

Richter, D. K., Meyer, S., Scholz, D., and Immenhauser, A.: Multiphase formation of Weichselian cryogenic calcites, Riesenberg Cave, NW Germany, Zeitschrift der Deutschen Gesellschaft für Geosciences, in review, 2012.

Růžičková, E. and Zeman, A.: The Blahutovice-1 borehole near Hranice na Moravě: weathering effects in Badenian deposits, Scripta, Geological Series (Masaryk University, Brno), 22, 128–132, 1992.

Šafanda, J. and Rajver, D.: Signature of the Last Ice Age in the present subsurface temperatures in the Czech Republic and Slovenia, Global Planet. Change, 29, 241–257, 2001.

Šafanda, J., Szewczyk, J., and Majorowicz, J.: Geothermal evidence of very low glacial temperatures on a rim of the Fennoscandian ice sheet, Geophys. Res. Lett., 31, L07211, doi:10.1029/2004GL019547, 2004.

Savchenko, E. B.: Mineral deposits on ice samples in the cave "Friendship", Peshchery (Caves), 16, 21–24, 1976.

Schimpf, D., Kilian, R., Kronz, A., Simon, K., Spötl, C., Wörner, G., Deininger, M., and Mangini, A.: The significance of chemical, isotopic, and detrital components in the three coeval stalagmites from the superhumid southernmost Andes (53° S) as high-resolution palaeoclimate proxies, Quaternary Sci. Rev., 30, 443–459, 2011.

Schmidt, F.-X.: Mineralogische Besonderheiten aus dem Höhlensystem Kreiselhalle-Malachitdom, in: Der Malachitdom. Ein Beispiel interdisziplinärer Höhlenforschung im Sauerland, Geologisches Landesamt Nordrhein-Westfalen, Krefeld, 91–104, 1992.

Scholz, D., Mühlinghaus, C., and Mangini, A: Modelling δ^{13}C and δ^{18}O in the solution layer on stalagmite surfaces, Geochim. Cosmochim. Acta, 73, 2592–2602, 2009

Skřivánek, F.: Jeskyně na Chlumu v Českém krasu, Československý kras, 7, 25–34, 1954.

Šmída, B.: Geomorfológia a genéza Plaveckého krasu ako modelového územia tzv. kontaktného krasu Západných Karpát s nižšou energiou reliéfotvorby, Ph. D. Thesis, Faculty of Natural Sciences, Comenius University in Bratislava, 220 pp., 2010.

Souchez, R. A. and Jouzel, J.: On the isotopic composition in δD and δ^{18}O of water and ice during freezing, J. Glaciol., 30, 369–372, 1984.

Souchez R. A. and Lorrain, R. D., Ice Composition and Glacier Dynamics, Springer Verlag, Berlin, 207 pp., 1991.

Souchez, R., Jouzel, J., Lorrain, R., Sleewaegen, S., Stiéverand, M., and Verbeke, V.: A kinetic isotope effect during ice formation by water freezing, Geophys. Res. Lett., 27, 1923–1926, 2000.

Spektor, V. B. and Spektor, V. V.: Karst processes and phenomena in the perennially frozen carbonate rocks of the Middle Lena River Basin, Permafrost Periglac., 20, 71–78, 2009.
Spötl, C.: Kryogene Karbonate im Höhleneis der Eisriesenwelt, Die Höhle, 59, 26–36, 2008.
Svendsen, J. I., Alexanderson, H., Astakhov, V. I., Demidov, I., Dowdeswell, J. A., Funder, S., Gataullin, V., Henriksen, M., Hjort, C., Houmark-Nielsen, M., Hubberten, H. W., Ingólfsson, Ó., Jakobsson, M., Kjær, K. H., Larsen, E., Lokrantz, H., Lunkka, J. P., Lyså, A., Mangerud, J., Matiouchkov, A., Murray, A., Möller, P., Niessen, F., Nikolskaya, O., Polyak, L., Saarnisto, M., Siegert, C., Siegert, M. J., Spielhagen, R. F., and Stein, R.: Late Quaternary ice sheet history of Northern Eurasia, Quaternary Sci. Rev., 23, 1229–1271, 2004.
Szewczyk, J. and Nawrocki, J.: Deep-seated relic permafrost in Northeastern Poland, Boreas, 40, 385–388, 2011.
Tulis, J. and Novotný, L.: System of Stratenská Cave, Osveta Publishers, Martin, 464 pp., 1989.
Urban, J. and Rzonca, B.: Karst systems analyzed using borehole logs – Devonian carbonates of the Świętokrzyskie (Holy Cross) Mountains, Central Poland, Geomorphology, 112, 27–47, 2009.
Urban, J. and Złonkiewicz, Z.: Wstępne wyniki badań geologicznych jaskini Chelosiowa Jama w Jaworzni koło Kielc, Geol. Q., 33, 367–369, 1989.
Vandenberghe, J.: Permafrost during the Pleistocene in north west and Central Europe, in: Permaforst response on economic development, environmental security and natural resources, Kluwer Acad. Publ., Dordrecht, The Netherlands, 185–194, 2001.
Viehmann, I.: Příspěvky k vývoji jeskynních perel (Un nouveau processus de génèse des perles de caverne), Československý Kras 12, 177–185, 1960.
Wrede, V.: Sinterschäden in der Großen Sunderner Höhle ein Beweis für Eisdruck?, Mitteilungen des Verbandes der deutschen Höhlen- und Karstforscher e. V. München, 45, 12–14, 1999.
Žák, K., Urban, J., Cílek, V., and Hercman, H.: Cryogenic cave calcite from several Central European caves: age, carbon and oxygen isotopes and a genetic model, Chem. Geol., 206, 119–136, 2004.
Žák, K., Onac, B. P., and Perşoiu, A.: Cryogenic carbonates in cave environments: a review, Quatern. Int., 187, 84–96, 2008.
Žák, K., Hercman, H., Orvošová, M., and Jačková, I.: Cryogenic cave carbonates from the Cold Wind Cave, Nízke Tatry Mountains, Slovakia: extending the age range of cryogenic cave carbonate formation to the Saalian, Int. J. Speleol., 38, 139–152, 2009.

Žák, K., Šmída, B., Filippi, M., Živor, R., Komaško, A., and Vybíral, S.: New localities of cryogenic cave carbonates in the Czech Republic and Slovakia, Speleofórum, Czech Speleol. Soc., 30, 103–110, 2011.

CPD
8, 2145–2185, 2012

Cryogenic cave carbonate

K. Žák et al.

Table 1. Characteristics of the studied caves. The U-series ages have been obtained in three different laboratories: Heidelberger Akademie der Wissenschaften, Heidelberg (H), Institute of Geological Sciences of Polish Academy of Sciences, Warsaw (W), Max-Planck-Institute for Chemistry, Mainz (M).

Cave number, name, country	Entrance position and elevation	Basic cave description, cave ventilation, etc.	Cave length, vertical extent (m)	CCC depth below surface	CCC age (U-series, ka)	References
1 Apostelhöhle, Germany	51°23′41″ N 8°40′02″ E 501 m a.s.l.	Complex maze of narrow, mostly vertical cavities, one narrow entrance (limited ventilation).	ca. 1000, 106	2 sites, 83 m and 93 m below entrance, ca. 50–60 m below the slope	37.53 ± 0.31 83.5 ± 1.4 408 + 42 – 31 35.59 ± 0.42	CCC description and dating: Richter et al. (2010b), dat. lab: H
2 Dechenhöhle, Germany	51°21′57″ N 7°38′40″ E 175 m a.s.l.	Mostly water-level controlled corridors, located at shallow depth, originally several entrances	870, ca. 13	one small site, ca. 20 m	not dated yet	CCC description: Richter and Niggemann (2005)
3 Glaseishöhle, Germany	47°30′44″ N 12°54′42″ E 2230 m a.s.l.	Alpine cave dominated by cavities extended in the vertical direction, stronger ventilation	2267, 229	229 m	not dated yet	CCC description: Richter et al. (2009c)
4 Großen Sunderner Höhle, Germany	51°18′45″ N 8°00′48″ E 280 m a.s.l.	Mostly water-level controlled cave with a large chamber at the crossing of fault-oriented corridors, moderate ventilation.	250, 42	28 m	not dated yet	CCC description: Richter et al. (2009a)
5 Heilenbecker Höhle, Germany	51°17′35″ N 7°20′34″ E 204 m a.s.l.	Complex cave of multistage origin, mostly developed as epiphreatic maze, narrow entrance, limited ventilation.	3822, 41	one site, about 25 m	31.25 ± 0.50	CCC description: Richter et al. (2008); dating: Richter et al. (2009b); dat. lab: H
6 Herbstlabyrinth-Adventhöhle, Germany	50°41′17″ N 8°12′23″ E 420 m a.s.l.	Extensive cave system, mostly sub-horizontal, large, water-level controlled corridors. Before discovery practically no ventilation. CCC in two areas, Rätselhalle (Site 1), and Weihnachtsbaum-Halle (Site 2)	5800, 80	Both sites are 30 to 40 m below surface	Site 1: 29.17 ± 0.48 28.70 ± 1.50 Site 2: 23.59 ± 0.30 23.96 ± 0.18	CCC description and dating: Rätselhalle – Kempe et al. (2006) and Richter et al. (2010a), Weihnachtsbaum-Halle: Richter et al. (2011); dat .lab: H
7 Malachitdom, Germany	51°27′56″ N 8°42′02″ E 424 m a.s.l.	Inclined cave with a large dome formed by corrosion, phreatic morphology, very limited communication with surface before discovery by quarrying	296, 58	two sites, ca 45 and 50 m below original surface	14.48 ± 0.12 14.84 ± 0.13 15.61 ± 0.20	CCC description: Erlenmeyer and Schudelski (1992), Schmidt (1992), Richter and Niggemann (2005), dating: Richter and Riechelmann (2008); dat. lab: H
8 Ostenberg Höhle, Germany	51°21′00″ N 8°24′00″ E 448 m a.s.l.	Cave system with three epiphreatic subhorizontal levels (CCC occurs in a main corridor of the middle level), limited ventilation before discovery.	622, 18	one site, 10 m below the surface	not dated yet	CCC description: Richter and Niggemann (2005); dat. lab: H
9 Riesenberghöhle, Germany	52°12′16″ N 9°17′16″ E 276 m a.s.l.	Epiphreatic cave system with a long subhorizontal water-elevel controlled corridors, before the discovery limited ventilation	1127, 20	Two sites, 30 to 40 m below the surface	66.4 ± 0.54 62.0 ± 0.4 61.6 ± 0.4 53.7 ± 0.3 11.9 ± 0.1 12.0 ± 0.1	CCC description and dating: this work and Richter et al. (2012), dating lab: M
10 BUML Cave, Czech Rep.	49°56′37″ N 14°07′42″ E 246 m a.s.l.	Phreatic cave with a large dome accessible only via long and narrow corridors, discovered by a quarry, limited ventilation.	274, 31	45 m	25.95 ± 1.53 33.77 ± 1.77	CCC description and dating: Žák et al. (2004); dating lab: W

CPD
8, 2145–2185, 2012

Table 1. Continued.

Cave number, name, country	Entrance position and elevation	Basic cave description, cave ventilation, etc.	Cave length, vertical extent (m)	CCC depth below surface	CCC age (U-series, ka)	References
11 Javořičko Caves, Czech Rep.	49°40′13″ N 16°54′49″ E 445 m a.s.l.	Extensive cave system developed in several levels, levels with CCC located relatively shallow below the surface	ca. 4000, 108	several sites, approximately 30 m	37.84 ± 0.73 38.09 ± 0.60 34.60 ± 0.41	CCC description: Žák et al. (2011), dating: this work; dating lab: H
12 Na Javorce Cave, Czech Rep.	49°56′17″ N 14°10′59″ E 330 m a.s.l.	Complicated extensive system of narrow shafts and corridors, very limited ventilation, discovered by excavation of sediment-filled narrow corridors	1634, 129	Site 1: 45 m, Site 2: 60 m, Site 3: 65 m	Site 1: 50.04 ± 0.59 28.56 ± 0.17 Site 2: 14.98 ± 0.17 Site 3: 9.191 ± 0.072	CCC description: Žák et al. (2011), dating: this work; dating lab: H
13 Novoroční (New Year) Cave, Czech Rep.	49°54′56″ N 14°03′48″ E 402 m a.s.l.	Smaller cave system developed by corrosion along faults, communication with surface only via narrow chimneys, originally sediment-filled, discovered by quarry	ca. 200, 32	one site, 60 m	34.26 ± 0.72	CCC description: Žák et al. (2011), dating: this work; dating lab: H
14 Portálová (Portal) Cave, Czech Rep.	49°56′58″ N 14°07′15″ E 242 m a.s.l.	Smaller cave system, almost completely sediment-filled, the CCC site was discovered by excavation of corridors, which were completely sediment-filled	ca. 180, 17	one site, 28 m	34.45 ± 0.34 34.01 ± 0.38	CCC description: Žák et al. (2011), dating: this work; dating lab: H
15 Hačova Cave, Slovakia	48°31′04″ N 17°23′33″ E 690 m a.s.l.	Small cave located in a hilly range, strong ventilation.	660, 73	one site, 45 m	47.58 ± 0.55	CCC description: Šmída (2010), Žák et al. (2011), dating: this work; dating lab: H
16 Mesačný tieň (Moon Shadow) Cave, Slovakia	49°13′00″ N 20°07′20″ E 1767 m a.s.l.	Large mountain cave system with only one CCC site. The cave has a strong ventilation. The deepest CCC site known so far.	ca. 26 000, 451	one site, 285 m below the closest surface	17.13 ± 0.12	CCC description: Žák et al. (2011), dating: this work, dating lab: H
17 Stratenská Cave, Slovakia	48°51′45″ N 20°18′50″ E 995 m a.s.l.	Extensive complex, multi-level cave system with large galleries and chambers, formed by allochthonous water streams. Could have larger ventilation in the past. Two CCC sites.	22 027, 194	two sites, ~ 120 m	22.61 ± 1.44 21.16 ± 2.66 23.43 ± 1.05	CCC description: Tulis and Novotný (1989), Hill and Forti (1997), description and dating: Žák et al. (2004); dating lab: W
18 Studeného vetra (Cold Wind) Cave, Slovakia	48°55′35″ N 19°39′19″ E 1678 m a.s.l.	Pre-Quaternary cave system with large domes, fossilized in the mountain range.	1518, 107	two sites, ca. 50–60 m	79.7 ± 2.3 104.0 ± 2.9 180.0 ± 6.3	CCC description and dating: Žák et al. (2009a); dating lab: W
19 Verných Cave, Slovakia	49°13′33″ N 20°10′16″ E 1522 m a.s.l.	An extensive cave system with relatively large corridors, moderate ventilation.	870, 50	one site, ca. 50 m	15.74 ± 0.47	CCC description: Orvošová and Vlček (2012); dating this work; dating lab: H
20 Cave System Jama Chelosiowa–Jaskinia Jaworznicka, Poland	50°51′33″ N 20°29′56″ E 257 m a.s.l.	Extensive cave system, mostly phreatic, numerous CCC sites. Before discovery no ventilation. Cave system is in an area of relatively flat surface.	3670, 59	ca. 12 sites, 33–43 m	36.0 ± 1.2 40.0 ± 1.3 38.8 ± 1.4 61.0 ± 1.8 53.0 ± 1.5	CCC description: Durakiewicz et al. (1995), description and dating: Žák et al. (2004), dating lab: W

CPD
8, 2145–2185, 2012
Cryogenic cave carbonate
K. Žák et al.

Table 2. New U-series data on CCC obtained in Heidelberg.

Lab. No.	Field No.	Sample location and description	^{234}U (initial) (‰)	^{238}U ($\mu g\,g^{-1}$)	^{232}Th ($ng\,g^{-1}$)	^{230}Th ($pg\,g^{-1}$)	Age (uncorr.) (ka)	Age (corr.) (ka)
5217	PORT1	Portálová Cave, Czech Republic, crystals and crystal aggregates	898.2 ± 6.5	8.6785± 0.0087	4.226± 0.022	74.59± 0.57	34.46	**34.45 ± 0.34**
5281	PORT2	Portálová Cave, Czech Republic, the same site, hemispheres	887.3 ± 5.3	6.5312± 0.0065	4.152± 0.032	55.19± 0.52	34.02	**34.01 ± 0.38**
5218	CJVK1	Na Javorce Cave, Czech Republic, Karakorum Section, flat rafts formed by clear yellowish crystals	1297.7 ± 4.0	5.2694± 0.0053	80.97± 0.31	46.79± 0.23	28.75	**28.56 ± 0.17**
5282	CJVK2	Na Javorce Cave, Czech Republic, the same site as CJVK1, flat rafts formed by white porous crystals	1364.7 ± 9.2	2.1741± 0.0054	28.89± 0.18	32.16± 0.27	50.18	**50.04 ± 0.59**
5256	CJVK3	Na Javorce Cave, Czech Republic, Půda Section (the deeper one), cave rafts, white	2304.6 ± 5.7	2.4009± 0.0024	30.60± 0.21	16.97± 0.19	15.09	**14.98 ± 0.17**
5257	MJAV1	Javoříčko Caves, Czech Republic, Olomouc Chamber, rafts formed by yellowish crystals	1144.7 ± 10.4	0.32932± 0.00066	8.627± 0.055	3.493± 0.056	38.17	**37.84 ± 0.73**
5283	MJAV2	Javoříčko Caves, Czech Republic, Olomouc Chamber, rafts, another site	1179.3 ± 7.7	0.5128± 0.0010	26.81± 0.14	5.578± 0.073	38.75	**38.09 ± 0.60**
5219	SHAC1	Hačova Cave, Slovakia, brownish crystals, partly skeletal aggregates	466.4 ± 5.2	0.9385± 0.0019	0.9655± 0.0039	8.122± 0.070	47.60	**47.58 ± 0.55**
5224	MEST1	Mesačný Tieň Cave, Slovakia, white crystal aggregates	183.9 ± 1.7	14.250± 0.014	41.27± 0.14	40.38± 0.25	17.20	**17.13 ± 0.12**
5515	NOVO1	Novoroční Cave, Czech Republic, one large white crystal aggregate	1451.8 ± 9.5	0.96340± 0.00190	1.946± 0.018	10.700± 0.190	34.28	**34.26 ± 0.72**
5516	VERJ1	Verných Cave, Slovakia, crystal aggregates, partly also cave rafts	1240.4 ± 9.6	1.1873± 0.0012	34.230± 0.340	6.020± 0.160	16.10	**15.74 ± 0.47**
5522	CJVK18	Na Javorce Cave, Czech Republic, cavity below the Půda Section (the deepest one), small white crystal aggregates	6955.9 ± 11.3	1.7141± 0.0017	21.65± 0.10	18.25± 0.14	9.236	**9.191 ± 0.072**
5523	MJAV3	Javoříčko Caves., Czech Republic, Ivošovy Caves section, large, brown-colored aggregates	1558.7 ± 14.8	1.6121± 0.0016	15.758± 0.085	18.88± 0.16	34.70	**34.60 ± 0.41**

CPD
8, 2145–2185, 2012

Table 3. New U-series data on CCC for the Riesenberghöhle, Germany, obtained in Mainz.

Sample (Riesenberghöhle)	^{238}U (µg g^{-1})	^{232}Th (ng g^{-1})	(^{234}U/^{238}U)	(^{230}Th/^{238}U)	Age (ka) uncorrected	Age (ka) corrected
"Zopfsinter" RieSe	2.75 ± 0.02	1.55 ± 0.02	1.7873 ± 0.0029	0.7163 ± 0.0028	53.7 ± 0.3	**53.7** ± **0.3**
"Zopfsinter-1", white	0.564 ± 0.005	2.20 ± 0.03	1.6201 ± 0.0029	0.7634 ± 0.0039	66.5 ± 0.5	**66.4** ± **0.5**
"Zopfsinter-1", brown	1.67 ± 0.01	2.69 ± 0.03	1.5620 ± 0.0029	0.1625 ± 0.0011	11.9 ± 0.1	**11.9** ± **0.1**
"Zopfsinter-2", white	1.41 ± 0.01	0.80 ± 0.01	1.5294 ± 0.0023	0.6784 ± 0.0030	61.6 ± 0.4	**61.6** ± **0.4**
Rhombohedric "Sinter-1", white	1.35 ± 0.01	2.89 ± 0.03	1.5254 ± 0.0025	0.6800 ± 0.0031	62.0 ± 0.4	**62.0** ± **0.4**
Rhombohedric "Sinter-1", brown	1.65 ± 0.01	7.23 ± 0.08	1.5626 ± 0.0026	0.1630 ± 0.0010	12.0 ± 0.1	**12.0** ± **0.1**

CPD
8, 2145–2185, 2012

Cryogenic cave carbonate

K. Žák et al.

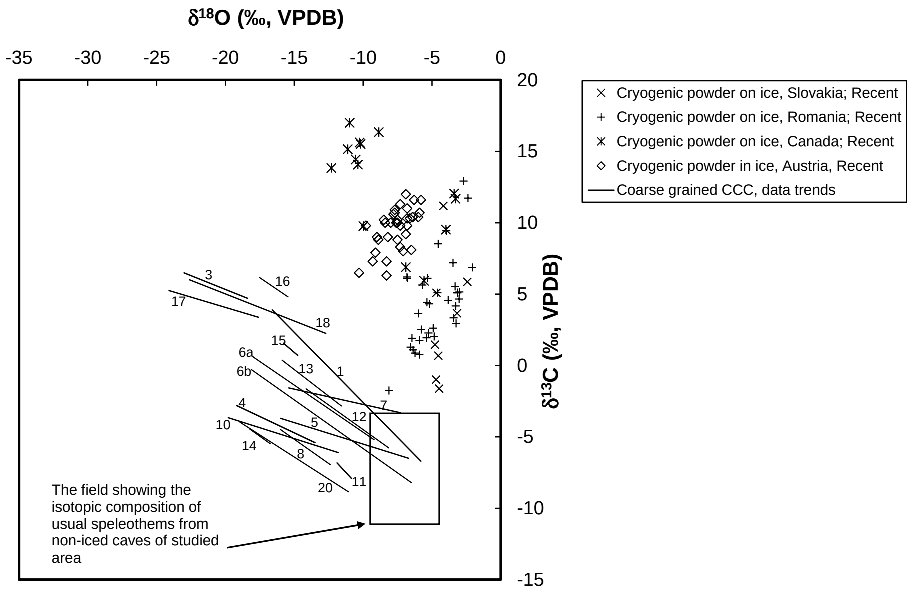

Fig. 1. Caption on next page.

Fig. 1. Stable isotope data of CCC. Data for different localities of coarse grained CCC are shown as a trend lines, calculated using linear regression. The regression lines were calculated for all analyses available from a given locality (single crystal bulk analyses, single aggregate bulk analyses, point analyses center to rim in larger crystals and crystal aggregates). The trends are directed towards lower $\delta^{18}O$ and higher $\delta^{13}C$ values as the freezing proceeds. Locality numbers are identical to Table 1 (Localities 2, 9, and 19 are not covered by published stable isotope data). Data sources: 1 – Apostelhöhle, Germany, Richter et al. (2010b); 3 – Glaseishöhle, Germany, Richter et al. (2009c); 4 – Großen Sunderner Höhle, Germany, Richter et al. (2009a); 5 – Heilenbecker Höhle, Germany, Richter et al. (2008, 2009b); 6a – Herbstlabyrinth, Germany, Rätselhalle, Richter et al. (2010a), 6b – the same cave, Weihnachtsbaumhalle, Richter et al. (2011); 7 – Malachitdom, Germany, Richter and Niggemann (2005), Richter and Riechelmann (2008); 8 – Ostenberg Höhle, Germany, Richter and Niggemann (2005); 10 – BUML Cave, Czech Republic, Žák et al. (2004); 11 – Javoříčko Caves, Czech Republic, Žák et al. (2011); 12 – Na Javorce Cave, Czech Republic, Žák et al. (2011); 13 – Novoroční Cave, Žák et al. (2011); 14 – Portálová Cave, Czech Republic, Žák et al. (2011); 15 – Hačova Cave, Slovakia, Žák et al. (2011); 16 – Mesačný tieň Cave, Slovakia, Žák et al. (2011); 17 – Stratenská Cave, Slovakia, Žák et al. (2004); 18 – Cold Wind Cave, Slovakia, Žák et al. (2009); 20 – Jama Chelosiowa-Jaskinia Jaworznicka, Poland, Žák et al. (2004). The data for cryogenic cave powder are from Clark and Lauriol (1992), Žák et al. (2004, 2008, 2011), Lacelle et al. (2009), Spötl (2008).

CPD
8, 2145–2185, 2012

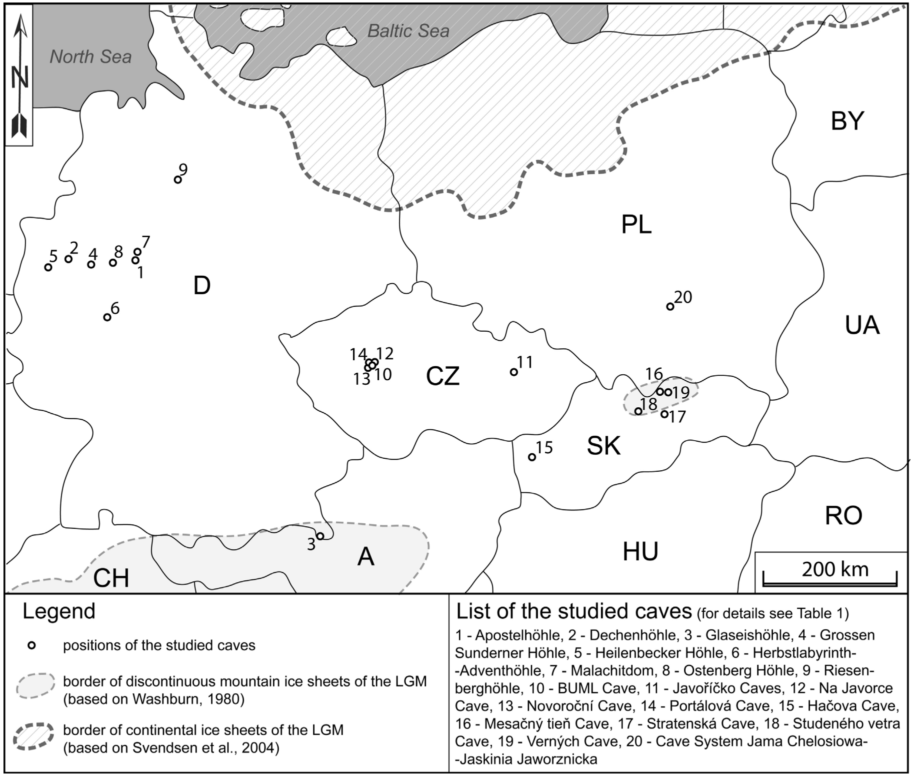

Fig. 2. Location of the studied caves within Central Europe. The limits of continental and Alpine mountain glaciation during the Last Glacial are taken from Washburn (1980) and Svendsen et al. (2004).

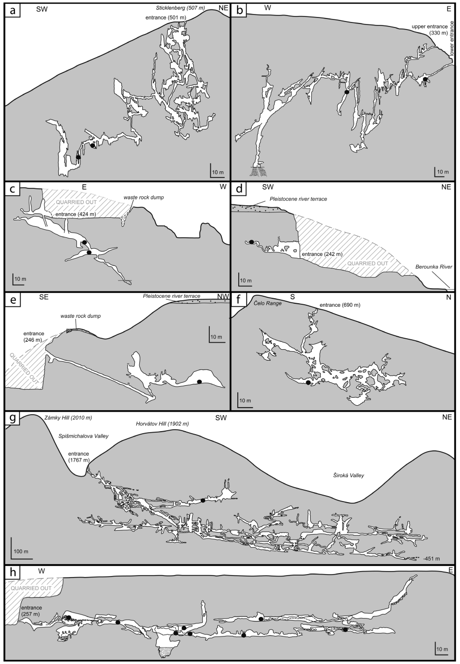

Fig. 3. Cave sections (projected profiles) of selected studied caves. CCC locations are indicated by black dots. **(a)** Apostelhöhle, Germany: mapping by M. Erlenmeyer and co-workers, section after Richter et al. (2010b); **(b)** Na Javorce Cave, Czech Republic: modified and redrawn after Dragoun et al. (2011), mapping by J. Dragoun, J. Vejlupek and J. Novotný; **(c)** Malachitdom, Germany: mapping and section after Erlenmeyer and Schudelski (1992); **(d)** Portálová Cave, Czech Republic: original drawing, mapping by J. Živor and co-workers; **(e)** BUML Cave, Czech Republic: original drawing, mapping by S. Martínek and P. Zbuzek; **(f)** Hačova Cave, Slovakia: original drawing by B. Šmída, mapping by B. Šmída, M. Hačo and co-workers; **(g)** Mesačný Tieň Cave, Slovakia: original drawing by B. Šmída, mapping by B. Šmída, I. Pap and co-workers; **(h)** Jama Chelosiowa – Jaskinia Jaworznica Cave System, Poland: mapping and section drawing by J. Gubała and A. Kasza, see also Urban and Rzonca (2009).

CPD
8, 2145–2185, 2012

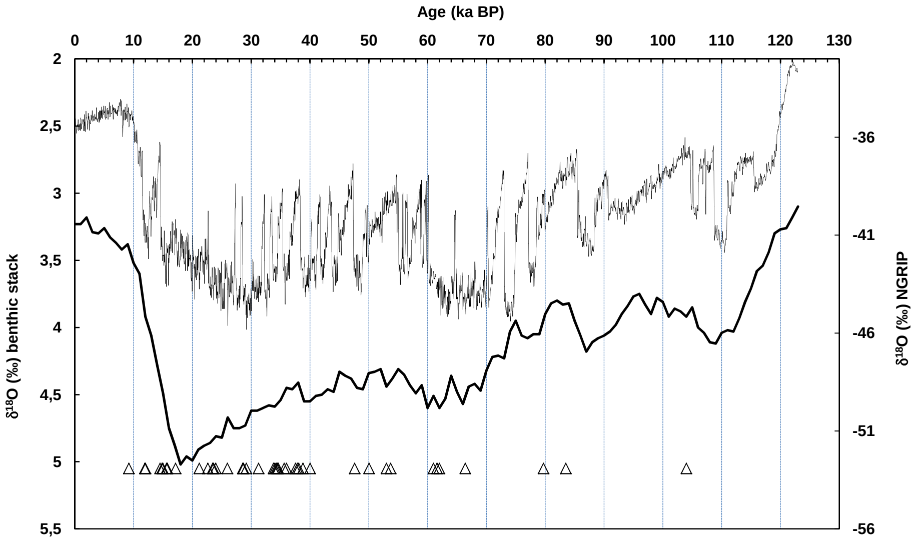

Fig. 4. Compilation of 42 ^{230}Th/U-age determinations of CCC from Germany, the Czech Republic, Slovakia and Poland for the last 123 ka. Age data are shown as triangles at randomly selected position versus vertical axis. Analytical errors of the age data are provided in Table 1 and are within the size of the symbols in most cases. The stacked benthic O isotope record of (Lisiecki and Raymo, 2005; thick line) serves as a reference curve for global glacial–interglacial climate variability. For the Northern Hemisphere climate the NGRIP record is shown (North Greenland Ice Core Members, 2004; thin line).

CPD
8, 2145–2185, 2012

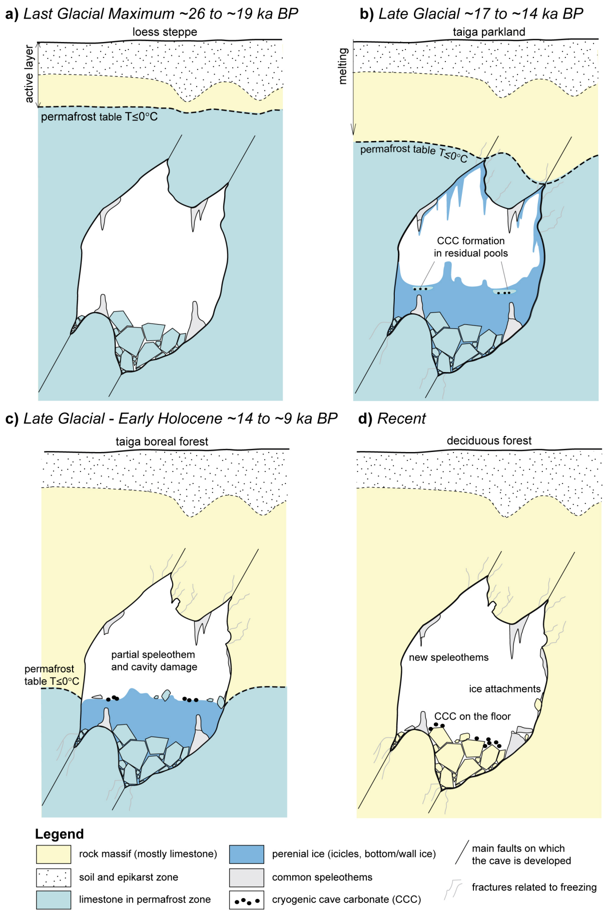

Fig. 5. Model of formation of CCC during single permafrost destruction (thawing) after the Last Glacial Maximum. See text for further details.